Huang et al., http://www.jcb.org/cgi/content/full/jcb.201209044/DC1

Figure S1. **F-actin dynamics in LAGFP and LAmGFP cells.** (A) Time-lapse images of LAGFP cells (MBY6656) grown in YES medium at 24°C. (B) Time-lapse images of LAmGFP (MBY7519) cells grown in YES medium at 24°C. In some images, the cell boundary is marked with dashed lines. Bars, 5 µm.

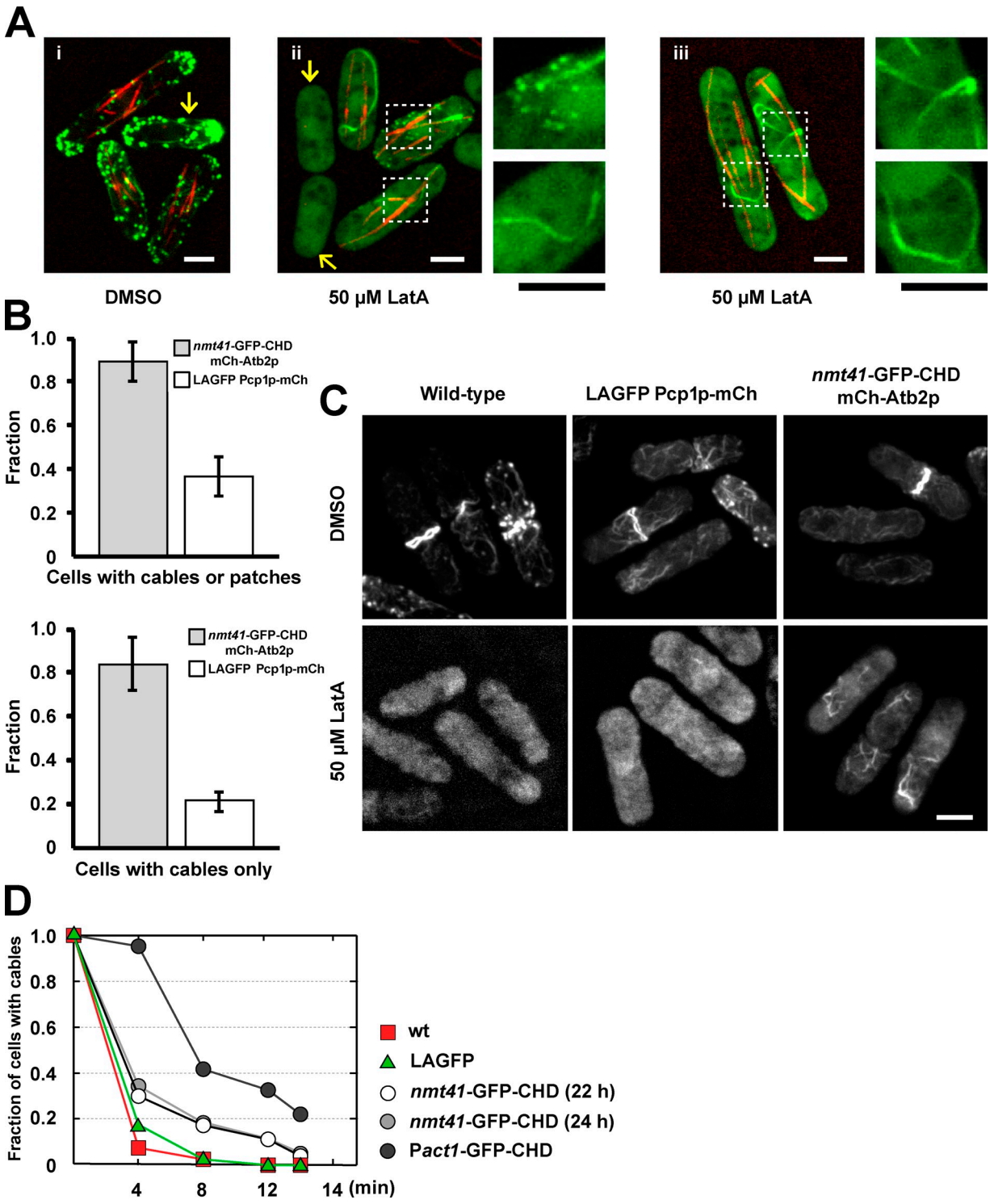

Figure S2. **The previously used marker, GFP-CHD, generates stabilized actin structures.** (A) Mixture of LAGFP Pcp1p-mCh cells (MBY6658) and *nmt41*-GFP-CHD mCh-Atb2p cells (MBY7132) treated with DMSO or LatA. *nmt41*-GFP-CHD mCh-Atb2p cells were induced in complete minimal medium for 22–24 h and mixed with equal amount of LAGFP Pcp1p-mCh cells just before LatA treatment. The mixing ensured that the LatA treatment regimen was identical in both strains. Live-cell images were taken immediately after LatA treatment for 12–30 min. DMSO was used as control and as a solution to dissolve LatA. White dashed boxes are enlarged on the right. Yellow arrows show the LAGFP Pcp1p-mCh cells, in which F-actin is more completely lost upon LatA treatment, compared with the GFP-CHD strain in which F-actin persists. (B) Graphs showing percentages of the indicated cells with aberrant F-actin structures after LatA treatment. LAGFP Pcp1p-mCh cells and 24-h induced *nmt41*-GFP-CHD mCh-Atb2p cells were mixed equally and treated with LatA for 12 min. All cells counted in this figure were live cells. Error bars show means ± SD of three independent experiments. In each experiment, >100 cells were counted for each strain. Top graph shows percentage of cells with either stabilized aberrant cables or patches. Bottom graph shows percentage of cells with only aberrant cables. (C) Images of DMSO- or LatA-treated, formaldehyde-fixed, and Alexa Fluor 488 phalloidin–stained wt (MBY192), LAGFP Pcp1p-mCh, and *nmt41*-GFP-CHD mCh-Atb2p cells, showing that the GFP-CHD–labeled aberrant structures in A were bona fide actin structures. All these LatA-treated and formaldehyde-fixed cells did not show any fluorescent structures before the staining by Alexa Fluor 488 phalloidin (not depicted). (D) Graphs showing percentage of the indicated cells with aberrant actin cables after LatA treatment. The results are the means of two independent experiments. In each experiment, 100 cells were counted for each data point. *nmt41*-GFP-CHD (MBY2309) were induced in complete minimal medium for 22 or 24 h. wt (MBY103), LAGFP (MBY7200), and P*act1*-GFP-CHD (MBY8043) cells were cultured in YES at 24°C overnight till mid–log phase. After LatA was added, cells were collected at 0, 4, 8, 12, and 14 min. Cells were then immediately fixed by paraformaldehyde and stained by Alexa Fluor 488 phalloidin for counting. For detailed description of LatA treatment and induction of *nmt41*-GFP-CHD containing cells, see Materials and methods. Bars, 3 µm.

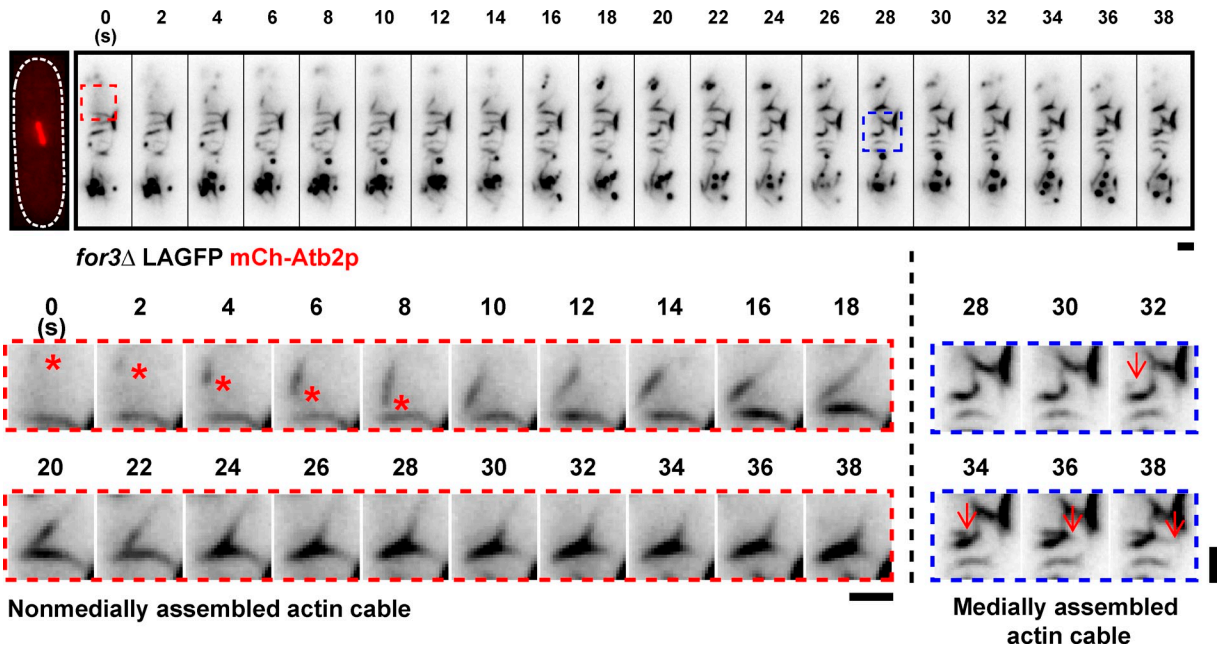

Figure S3. **Mitotic actin cable assembly can be observed in both medial region and nonmedial region in the *for3*Δ LAGFP mCh-Atb2p cell.** Time-lapse TIRFM images of a representative *for3*Δ LAGFP mCh-Atb2p cell (MBY7004) at 24°C. The first image of the top row shows the appearance of the spindle before the video was started. Bottom red images on the left show the magnified time-lapse images of the red dashed box, starting from time 0. The red asterisks trace the movement of a single nonmedially assembled actin cable. Bottom blue images on the right show the magnified time-lapse images of the blue dashed box. The red arrows trace the movement of a single medially assembled actin cable. In some images, the cell boundary is marked with dashed lines. Bars, 2 μm.

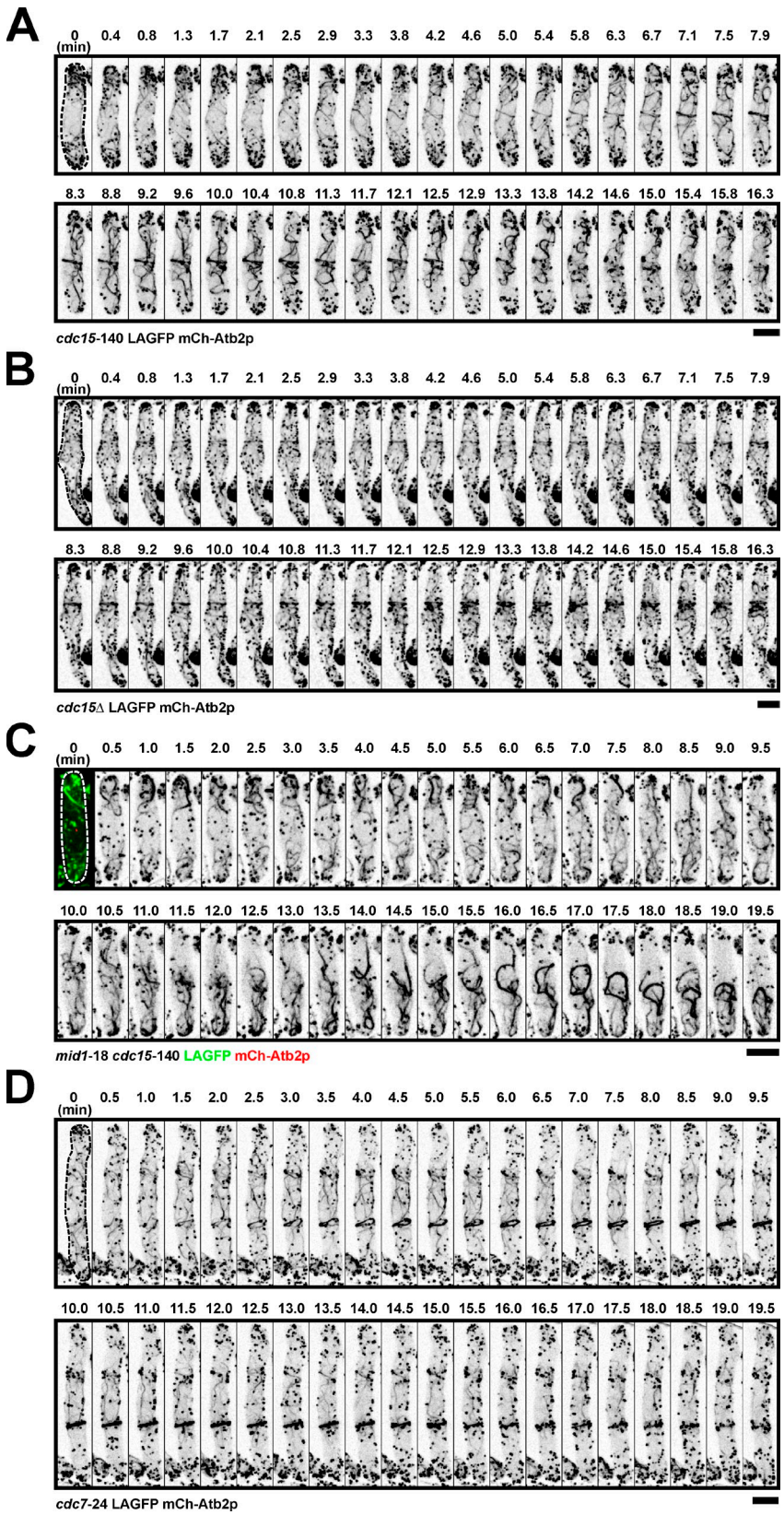

Figure S4. **The assembly of mitotic actin cables is independent of Cdc15p, Mid1p, or Cdc7p.** (A) Time-lapse images of a representative mitotic *cdc15*-140 LAGFP mCh-Atb2p cell (MBY7133) at 36°C. (B) Time-lapse images of a representative mitotic *cdc15Δ* LAGFP mCh-Atb2p cell (MBY7166) at 24°C. Cell was germinated from spore. (C) Time-lapse images of a representative mitotic *mid1*-18 *cdc15*-140 LAGFP mCh-Atb2p cell (MBY7160) at 36°C. (D) Time-lapse images of a representative mitotic *cdc7*-24 LAGFP mCh-Atb2p (MBY7179) cell at 36°C. In some images, the cell boundary is marked with dashed lines. Bars, 5 µm.

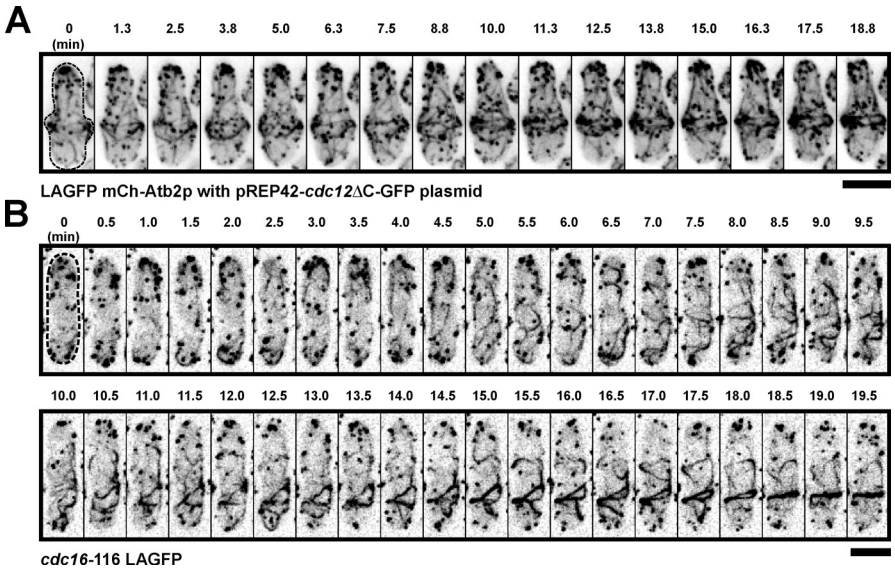

Figure S5. **The movement of nuclei is not required for the migration of actin cables to the cell division site.** (A) Time-lapse images of a representative interphase LAGFP mCh-Atb2p cell overexpressing pREP42-*cdc12*ΔC-GFP (MBY7228). Cells were cultured in minimal medium lacking uracil (ura−) with thiamine to mid–log phase. Then, cells were induced in medium without thiamine for 25 h before imaging. (B) Time-lapse images of a representative HU-arrested interphase *cdc16*-116 LAGFP cell (MBY7629) at 36°C. For detailed description of HU treatment, please see Materials and methods. In some images, the cell boundary is marked with dashed lines. Bars, 5 µm.

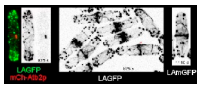

Video 1. **Actin dynamics in LAGFP mCh-Atb2p, LAGFP, and LAmGFP cells.** Images were acquired by optimized time-lapse spinning-disk microscopy (Axiovert 200M microscope) at 24°C. (left) Frames were collected every 25 s. Related to Fig. 2 A. (middle) LAGFP is in black. Frames were collected every 25 s. The red asterisk points out the cell in Fig. S1 A. Related to Fig. S1 A. (right) LAmGFP is in black. Frames were collected every 30 s. Related to Fig. S1 B. For the whole video, frame rate is six frames per second.

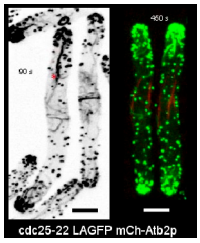

Video 2. **Nonmedially assembled actin cables migrate toward the middle in *cdc25*-22 LAGFP mCh-Atb2p cells.** Images were either acquired by time-lapse spinning-disk microscopy (left; Eclipse Ti microscope; *micro*LAMBDA) or an optimized time-lapse spinning-disk microscopy (right; Axiovert 200M microscope) at 24°C. (left) LAGFP is in black. Frames were collected every 5 s. Red asterisks show nonmedially assembled actin cables migrating to the medial region during ring assembly. Related to Fig. 2 B. (right) LAGFP is in green, and mCh-Atb2p is in red. Frames were collected every 15 s. Yellow asterisks show nonmedially assembled actin cables migrating to the medial region during ring assembly. Bars, 5 µm. For the whole video, frame rate is five frames per second.

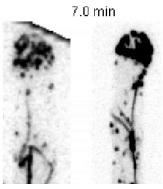

Video 3. **Actin cables migrated from the nonmedial region toward the middle during ring assembly in *nmt1-wee1*-50 *adf1*-1 LAGFP cells.** Images were either acquired by time-lapse spinning-disk microscopy (right; Eclipse Ti microscope; *micro*LAMBDA) or an optimized time-lapse spinning-disk microscopy (left; Axiovert 200M microscope) at 36°C. LAGFP is in black. Red asterisks show cables migrating from the nonmedial region to the cell middle. In both images, frames were collected every 30 s. Related to Fig. 2 D. Bars, 5 µm. For the whole video, frame rate is three frames per second.

Video 4. **TIRF video of actin dynamics in a mitotic LAGFP mCh-Atb2p cell.** Images were acquired by a customized time-lapse TIRFM (TILL Photonics based on an automated iMic stand and an Olympus 1.45 NA 100× objective) at 24°C. Frames were collected every 2 s. Related to Fig. 2 I. For the whole video, frame rate is 15 frames per second.

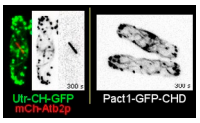

Video 5. **Nonmedial actin cables can also be observed in wt cells expressing Utr-CH-GFP mCh-Atb2p or P*act1*-GFP-CHD.** Images were either acquired by time-lapse spinning-disk microscopy (right; Eclipse Ti microscope; *micro*LAMBDA) or an optimized time-lapse spinning-disk microscopy (left; Axiovert 200M microscope) at 24°C. (left) Related to Fig. 4 A. (right) P*act1*-GFP-CHD is in black. Related to Fig. 4 E. In both panels, frames were collected every 25 s. For the whole video, frame rate is six frames per second.

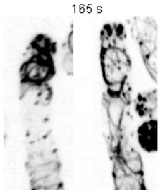

Video 6. **Nonmedial actin cables migrate toward the middle *cdc25*-22 P*act*1-GFP-CHD mCh-Atb2p cells.** Images were acquired by time-lapse spinning-disk microscopy (Eclipse Ti microscope; *micro*LAMBDA) at 24°C. LAGFP is in black. Red asterisks show cables migrating from the nonmedial region toward the middle. Frames were collected every 15 s. Related to Fig. 4 F. Bars, 5 µm. For the whole video, frame rate is three frames per second.

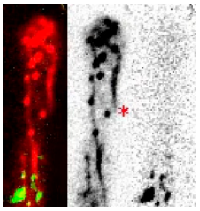

Video 7. **Nonmedial actin cables migrate toward the middle in released *cdc25*-22 Rlc1p-3GFP LAmCh cell.** Single-plane images were acquired by time-lapse spinning-disk microscopy (Nikon ECLIPSE Ti microscope; *micro*LAMBDA) at 24°C. LAmCh is in red, and Rlc1p-3GFP is in green. Red asterisks show the migration of a nonmedial cable toward the middle. Frames were collected every 1.3 s. Related to Fig. 5 A. For the whole video, frame rate is six frames per second.

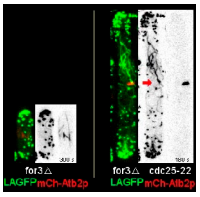

Video 8. **Actin dynamics in *for3Δ*-related cells.** Images were acquired by an optimized time-lapse spinning-disk microscopy (Axiovert 200M microscope) at 24°C. (left) *for3Δ* LAGFP mCh-Atb2 cell. Frames were collected every 25 s. Related to Fig. 6 A. (right) *cdc25*-22 *for3Δ* LAGFP mCh-Atb2p cell. Red arrows show a nonmedially assembled actin cable migrating toward the middle region during ring assembly. Frames were collected every 15 s. Related to Fig. 6 B. For the whole video, frame rate is five frames per second.

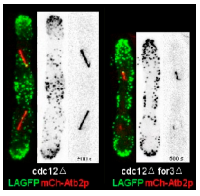

Video 9. **Mitotic actin cables are either not prominent or not detectable during mitosis in *cdc12Δ* LAGFP mCh-Atb2p cell or *for3Δ cdc12Δ* LAGFP mCh-Atb2p cell.** (left) *cdc12Δ* LAGFP mCh-Atb2p cell; (right) *for3Δ cdc12Δ* LAGFP mCh-Atb2p cell. Images were acquired by optimized time-lapse spinning-disk microscopy (Axiovert 200M microscope) at 24°C. In both images, cells were germinated from spores. In both images, frames were collected every 25 s. For the whole video, frame rate is 10 frames per second. Related to Fig. 6 (J–L).

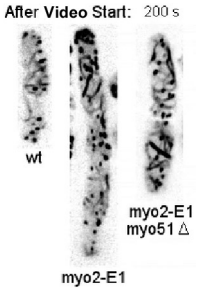

Video 10. **Single-plane videos of LAGFP mCh-Atb2p, *myo2*-E1 LAGFP mCh-Atb2p, and *myo2*-E1 *myo51Δ* LAGFP mCh-Atb2p cells.** Single-plane images were acquired by time-lapse spinning-disk microscopy (Eclipse Ti microscope; *micro*LAMBDA) at 36°C. Cells were shifted to 36°C for 4 h before imaging. Differential interference contrast and mCh-Atb2p (red) images of the cells were taken before the start of the videos. LAGFP is shown in black. In all images, frames were collected every 5 s. For the whole video, frame rate is 10 frames per second. Related to Fig. 8 (D and E).

Table S1. ***S. pombe* strains used in this study**

Strain	Relevant genotype	Source
MBY50	*cdc3*-124 *ade6*-216 *ura4*-D18 *leu1*-32 h$^+$	Laboratory collection
MBY102	*ade6*-210 *ura4*-D18 *leu1*-32 h$^+$	Laboratory collection
MBY103	*ade6*-210 *ura4*-D18 *leu1*-32 h$^-$	Laboratory collection
MBY112	*cdc8*-110 *ade6*-210 *ura4*-D18 *leu1*-32 *his3*Δ h$^+$	Laboratory collection
MBY144	*cdc12*-112 *ura4*-D18 *leu1*-32 h$^-$	Laboratory collection
MBY151	*myo2*-E1 *ura4*-D18 *leu1*-32 h$^-$	Laboratory collection
MBY169	*wee1*-50 *leu1*-32 h$^-$	Laboratory collection
MBY192	*ura4*-D18 *leu1*-32 h$^-$	Laboratory collection
MBY341	*rng3-65 ade6*-210 *ura4*-D18 *leu1*-32 h$^-$	Laboratory collection
MBY1241	*cdc25*-22 *ura4*-D18 *leu1*-32 *his7*-366 h$^-$	Laboratory collection
MBY2309	*nmt41*-GFP-CHD::*leu1*$^+$ *ade6*-216 *ura4*-D18 *leu1*-32 h$^-$	Laboratory collection
MBY4678	*adf1*-1::*ura4*$^+$ *ade6*-210 *ura4*-D18 *leu1*-32 h$^-$	From K. Nakano[a]
MBY5856	mCh-*atb2*::*hph ura4*-D18 *leu1*-32 h$^-$	Laboratory collection
MBY6247	*cdc12*-3Venus::*kanMX6 ura4*-D18 *leu1*-32 h$^+$	From I. Mabuchi[b]
MBY6248	*cdc12*-3Venus::*kanMX6 ura4*-D18 *leu1*-32 h$^-$	From I. Mabuchi
MBY6656	P*act1*-LAGFP::*leu1*$^+$ *ura4*-D18 *leu1*-32 h$^-$	This study
MBY6658	P*act1*-LAGFP::*leu1*$^+$ *pcp1*-mCh::*ura4*$^+$ *leu1*-32 h$^-$	This study
MBY6659	P*act1*-LAGFP::*leu1*$^+$ mCh-*atb2*::*hph ura4*-D18 *leu1*-32 h$^-$	This study
MBY6787	*kanMX6-nmt1-wee1*-50 *ura4*-D18 *leu1*-32 h$^-$	This study
MBY6843	P*act1*-LAmCh::*leu1*$^+$ *ade6*-216 *ura4*-D18 *leu1*-32 h$^+$	This study
MBY6844	P*act1*-LAmCh::*leu1*$^+$ *ade6*-216 *ura4*-D18 *leu1*-32 h$^-$	This study
MBY6866	*adf1*-1::*ura4*$^+$ *kanMX6-nmt1-wee1*-50 P*act1*-LAGFP::*leu1*$^+$ h$^-$	This study
MBY6914	P*act1*-LAmCh::*leu1*$^+$ *cdc12*-3Venus::*kanMX6* h$^+$	This study
MBY6916	*cdc25*-22 P*act1*-LAGFP::*leu1*$^+$ mCh-*atb2*::*hph leu1*-32 h$^+$	This study
MBY6955	*cdc25*-22 P*act1*-LAmCh::*leu1*$^+$ *rlc1*-3GFP::*kanMX6* h$^-$	This study
MBY6988	*cdc25*-22 P*act1*-LAmCh::*leu1*$^+$ *cdc12*-3Venus::*kanMX6*	This study
MBY6996	*cdc8*-110 P*act1*-LAGFP::*leu1*$^+$	This study
MBY7004	*for3*Δ::*kanMX6* P*act1*-LAGFP::*leu1*$^+$ mCh-*atb2*::*hph leu1*-32 h$^+$	This study
MBY7006	*for3*Δ::*kanMX6 cdc25*-22 P*act1*-LAGFP::*leu1*$^+$ mCh-*atb2*::*hph leu1*-32	This study
MBY7103	*mid1*Δ::*ura4*$^+$ P*act1*-LAGFP::*leu1*$^+$ mCh-*atb2*::*hph leu1*-32	This study
MBY7114	P*act1*-LAGFP::*leu1*$^+$ mCh-*atb2*::*hph ura4*-D18 *leu1*-32 h$^+$	This study
MBY7132	*nmt41*-GFP-CHD::*leu1*$^+$ mCh-*atb2*::*hph leu1*-32 h$^-$	This study
MBY7133	*cdc15*-140 P*act1*-LAGFP::*leu1*$^+$ mCh-*atb2*::*hph leu1*-32	This study
MBY7154	*myo51*Δ::*ura4*$^+$ *ade6*-210 *ura4*-D18 *leu1*-32 h$^+$	From D.P. Mulvihill[c]
MBY7160	*mid1*-18 *cdc15*-140 P*act1*-LAGFP::*leu1*$^+$ mCh-*atb2*::*hph leu1*-32	This study
MBY7161	*mid1*-18 P*act1*-LAGFP::*leu1*$^+$ mCh-*atb2*::*hph leu1*-32	This study
MBY7166	*cdc15*Δ::*ura4*$^+$/*cdc15*$^+$ P*act1*-LAGFP::*leu1*$^+$ mCh-*atb2*::*hph ura4*-D18/*ura4*-D18 *leu1*-32/*leu1*-32 h$^+$/h$^-$	This study
MBY7167	*cdc8*Δ::*ura4*$^+$/*cdc8*$^+$ P*act1*-LAGFP::*leu1*$^+$ mCh-*atb2*::*hph ura4*-D18/*ura4*-D18 *leu1*-32/*leu1*-32 h$^+$/h$^-$	This study
MBY 7176	*cdc12*Δ::*ura4*$^+$/*cdc12*$^+$ P*act1*-LAGFP::*leu1*$^+$ mCh-*atb2*::*hph ura4*-D18/*ura4*-D18 *leu1*-32/*leu1*-32 h$^+$/h$^-$	This study
MBY7179	*cdc7*-24 P*act1*-LAGFP::*leu1*$^+$ mCh-*atb2*::*hph*	This study
MBY7200	P*act1*-LAGFP::*leu1*$^+$ *ade6*-216 *ura4*-D18 *leu1*-32 h$^-$	This study
MBY7228	P*act1*-LAGFP::*leu1*$^+$ mCh-*atb2*::*hph* (MBY6659) + *pREP42-cdc12*Δ*C*-GFP (pAY25, *ura4*$^+$)	This study (plasmid from F. Chang[d])
MBY7244	P*act1*-LAmCh::*leu1*$^+$ *cdc12*-3GFP::*kanMX6* h$^-$	This study
MBY7277	*cdc3*Δ::*ura4*$^+$/*cdc3*$^+$ P*act1*-LAGFP::*leu1*$^+$ mCh-*atb2*::*hph ura4*-D18/*ura4*-D18 *leu1*-32/*leu1*-32 h$^+$/h$^-$	This study
MBY7385	*myo2*-E1 *myo51*Δ::*ura4*$^+$ *leu1*-32	This study
MBY7465	*cdc12*Δ::*ura4*$^+$/*cdc12*$^+$ *for3*Δ::*kanMX6*/*for3*$^+$ P*act1*-LAGFP::*leu1*$^+$ mCh-*atb2*::*hph ura4*-D18/*ura4*-D18 *leu1*-32/*leu1*-32 h$^+$/h$^-$	This study
MBY7519	P*act1*-LAmGFP::*leu1*$^+$ *ade6*-210 *ura4*-D18 *leu1*-32 h$^+$	This study
MBY7521	*cdc25*-22 *for3*Δ::*kanMX6 ura4*-D18	This study
MBY7629	*cdc16*-116 P*act1*-LAGFP::*leu1*$^+$ *leu1*-32	This study
MBY7867	P*act1*-Utr-CH-GFP::*leu1*$^+$ mCh-*atb2*::*hph*	This study
MBY7992	*cdc3*-124 P*act1*-LAGFP::*leu1*$^+$	This study
MBY7993	*cdc25*-22 P*act1*-LAGFP::*leu1*$^+$ *rlc1*-mCh::*ura4*$^+$	This study
MBY7996	*cdc16*-116 *cdc12*-112 P*act1*-LAGFP::*leu1*$^+$ *leu1*-32	This study

Table S1. ***S. pombe* strains used in this study** *(Continued)*

Strain	Relevant genotype	Source
MBY7998	*cdc12*-3Venus::*kanMX6* mCh-*atb2*::*hph ura4*-D18 *leu1*-32 h^+	This study
MBY8025	P*act1*-GFP::*leu1*$^+$ *ade6*-216 *ura4*-D18 *leu1*-32 h^-	This study
MBY8029	*myo51*Δ::*ura4*$^+$ *cdc12*-3Venus::*kanMX6* mCh-*atb2*::*hph*	This study
MBY8031	*myo2*-E1 *cdc12*-3Venus::*kanMX6* mCh-*atb2*::*hph*	This study
MBY8033	*myo2*-E1 *myo51*Δ::*ura4*$^+$ *cdc12*-3Venus::*kanMX6* mCh-*atb2*::*hph*	This study
MBY8043	P*act1*-GFP-CHD (1–189 aa)::*leu1*$^+$ *ade6*-216 *ura4*-D18 *leu1*-32 h^-	This study
MBY8149	*cdc25*-22 P*act1*-GFP-CHD (1–189 aa)::*leu1*$^+$ mCh-*atb2*::*hph*	This study

[a]University of Tsukuba, Tsukuba, Japan.
[b]Gakushuin University, Tokyo, Japan.
[c]University of Kent, Kent, England, UK.
[d]Columbia University, New York, NY.